ISSN 1063-7745, Crystallography Reports, 2017, Vol. 62, No. 2, pp. 260–264. © Pleiades Publishing, Inc., 2017.

NANOMATERIALS, CERAMICS

Non-Isothermal Crystallization Kinetics of Fe_2O_3–CaO–SiO_2 Glass Containing Nucleation Agent P_2O_5/TiO_2[1]

Bin Li[a,*], Yongya Wang[a], Wenqin Luo[a], Jingfen Li[a], and Jianyou Li[b]

[a] *Department of Material Chemistry, Huzhou University, Huzhou 313000, China*

[b] *Orthopedic Department, Huzhou Central Hospital, Huzhou 313000, China*

**e-mail: stra_ceo@163.com*

Received November 18, 2015

Abstract—Fe_2O_3–CaO–SiO_2 glass ceramics containing nucleation agent P_2O_5/TiO_2 were prepared by sol-gel method. The samples were characterized by X-ray diffraction (XRD) and differential scanning calorimetry (DSC). The activation energy and kinetic parameters for crystallization of the samples were calculated by the Johnson-Mehi-Avrami (JMA) model and Augis-Bennett method according to the results of DSC. The results showed that the crystallization mechanism of Fe_2O_3–CaO–SiO_2 glass, whose non-isothermal kinetic parameter $n = 2.3$, was consistent with surface crystallization of the JMA model. The kinetics model function of Fe_2O_3–CaO–SiO_2 glass, $f(\alpha) = 2.3(1 - \alpha)[-\ln(1 - \alpha)]^{0.57}$, was also obtained. The addition of nucleation agent P_2O_5/TiO_2 could reduce the activation energy, which made the crystal growth modes change from one-dimensional to three-dimensional.

DOI: 10.1134/S1063774517020080

INTRODUCTION

Magnetic mediated hyperthermia (**MMH**) was a new cancer therapy developed in recent years. Fe_2O_3–CaO–SiO_2 glass ceramics, due to their strong magnetism and good biological activity, were widely concerned by researchers. So MMH using Fe_2O_3–CaO–SiO_2 ferromagnetic glass ceramics prepared by melting method had made great progress in animal experiments [1–3]. The Fe_2O_3–CaO–SiO_2 glass ceramics as bioactive material had also been prepared by sol-gel method [4]. Glass ceramics prepared by sol-gel method were of higher purity, more specific surface area and inherent porous nature at low reaction temperature [5, 6], thus sol-gel method was widely applied to the preparation of new glass ceramics.

Glass ceramics were prepared by controlled crystallization, so the crystallization kinetics and mechanism of nucleation and growth were the key factors to optimize the processing parameters for desired product [7]. While activation energy and crystallization mechanisms were the most important kinetic parameters for the crystallization of glasses, which can be obtained by differential thermal analysis (DTA) and differential scanning calorimetry (DSC) results [8–11]. A variety of non-isothermal theoretical models were proposed to explain the crystallization kinetics of glasses, and several models were frequently used to identify the non-isothermal crystallization mechanism in the previous works [12–15]. The results indicated that effects of different nucleation agent on the crystallization kinetics parameters were different, appropriate nucleation agent could reduce the activation energy, increase the crystallization growth index and promote the occurence of bulk crystallization. Stookey believed that efficient internal nucleation of glass enabled the development of homogeneous and fine-grained microstructure [16]. The effect of nucleating agents TiO_2 and P_2O_5 on the controlled crystallization process of glass had been discussed [17–19]. However, the effect of TiO_2 and P_2O_5 on the crystallization of Fe_2O_3–CaO–SiO_2 glass ceramics had not been investigated.

The crystallization mechanisms of Fe_2O_3–CaO–SiO_2 glass ceramics prepared by sol-gel method were discussed in present work. A series of DSC under non-isothermal conditions were carried out at various heating rates so as to determine the crystallization kinetic parameters and the kinetics model function. Then the crystallization kinetic parameters of the samples containing nucleation agent TiO_2 and P_2O_5 were also calculated on the base of the above results to analyze the effect of nucleation agent on the crystallization of Fe_2O_3–CaO–SiO_2 glass ceramics, which could provide some theoretical support to the preparation of Fe_2O_3–CaO–SiO_2 glass ceramic containing nucleation agent.

[1] The article is published in the original.

EXPERIMENTAL

Glass sample *B*1 with composition 19.2CaO–7.24SiO_2–2.1Fe_2O_3 while samples *B*2 and *B*3 have the basic composition with 1 wt% of the nucleator TiO_2/P_2O_5 in excess of 100% were prepared. The solution of tetraethyl orthosilicate (TEOS) and ethanol were prepared. Distilled water was added in the solution, the molar ratio of TEOS and water was 1 : 15. Then hydrochloric acid was added in the solution and stirred with a magnetic stirrer for 10 min before the calcium nitrate and iron nitrate were added in the solution. The resulting solution was then transferred into water bath box and maintained at 45°C for 150 min. Then the temperature was raised up to 65°C until colloidal tilt lost liquidity. The samples were aged for 7 days at room temperature. The gels obtained were baked in the drying oven at 120°C for 12 h, and were heated at 550°C for 1 h in a heat treatment furnac, then slowly cooled to room temperature, the mass glasses were obtained. The glass samples were ground into powder and measured by DSC. The nucleation and crystal growth temperature ranges can be fixed according to the DSC curve. At last the samples were heat-treated for 1h in atmosphere.

X-ray diffraction (XRD) analysis was performed with a XD-6 X-ray diffractometer at room temperature, with CuK_α radiation, 36 kV voltage and 20 mA current. X-ray data were collected in the $5 < 2\theta < 80$ range. Prior to the XRD test, the samples were ground into powder and filtered through 300-mesh gauze. The XRD patterns were then compared with those in the Joint Committee on Powder Diffraction Standards (JCPDS).

The samples were characterized by DSC using SDT-Q600 differential thermal scanning analyzer. The sample weight was about 10.00 mg, and alumina was used as reference. The temperature range of collected data was 500~1100°C in the air.

THEORETICAL ANALYSIS

The isothermal crystallization process in glasses were usually described by the JMA equation [20, 21],

$$\alpha = 1 - \exp[-(kt)^n], \quad (1)$$

where α is the crystallized fraction which is crystallized at time t, n is the Avrami exponent which depends on the mechanism of the growth and dimensionality of crystal, k is a rate constant that follows an Arrhenius equation

$$k = k_0 \exp(-E/RT), \quad (2)$$

where k_0 is the pre-exponential factor, E is the activation energy. Taking the first derivative of α with respect to t, the rate equation can be obtained

$$\frac{d\alpha}{dt} = (1-\alpha)nk^n t^{n-1}, \quad (3)$$

and eliminating t by α from Eq. (1)

$$\frac{d\alpha}{dt} = (1-\alpha)nk[-\ln(1-\alpha)]^{(n-1)/n}. \quad (4)$$

Which can be expressed as the product of $k(T)$ and $f(\alpha)$

$$\frac{d\alpha}{dt} = k(T)f(\alpha). \quad (5)$$

Where

$$f(\alpha) = n(1-\alpha)[-\ln(1-\alpha)]^{(n-1)/n}. \quad (6)$$

Where $k(T)$ is temperature dependent rate constant, $f(\alpha)$ is the kinetics model function related to the mechanism.

The DTA was carried with a constant heating rate, the temperature changed linearly with time

$$T = T_0 + \beta t, \quad (7)$$

where T_0 is the temperature at which the crystallization begins and T is the temperature at time t, β is the heating rate. For non-isothermal process, according to Eq. (2) and Eq. (7), Eq. (1) can be written as

$$\alpha = 1 - \exp\left[-\left(k_0 \exp\left(-\frac{E}{R}\right)\right)^n \left(\frac{T-T_0}{\beta}\right)^n\right], \quad (8)$$

Eq. (5) can be written as

$$\frac{d\alpha}{dt} = \frac{k_0}{\beta}\exp\left(-\frac{E}{RT}\right)f(\alpha). \quad (9)$$

In this work the composite integral method [22, 23] was based on the Coats–Redfern equation [24], which was rewritten as follows

$$\ln\left(\beta\frac{g(\alpha)}{T^2}\right) = \ln\left(\frac{k_0 R}{E}\right) - \frac{E}{RT}, \quad (10)$$

where $g(\alpha)$ is the integral expression of the kinetics model function

$$g(\alpha) = \int_0^\alpha \frac{d\alpha}{f(\alpha)}. \quad (11)$$

So the curve $\ln(\beta g(\alpha)/T^2)$ vs. $1/T$ for a given analytical form of $g(\alpha)$ should be a straight line at different heating rates. Then the kinetic model $f(\alpha)$ that gives the best correlation coefficient was chosen, for which the data fall in a single master straight line. The activation energy E and non-isothermal kinetic parameter n can be calculated from Augis-Bennett approximation method [25, 26]

$$\ln\left(\frac{\beta}{T_p - T_0}\right) = \ln k_0 - \frac{E}{RT_p}, \quad (12)$$

$$n = \frac{2.5}{\Delta T}\frac{RT_p^2}{E}. \quad (13)$$

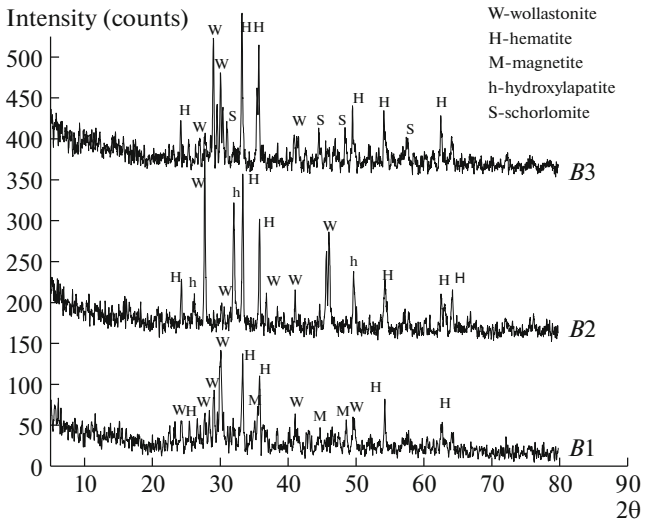

Fig. 1. XRD patterns of the glass samples heated at 850°C.

Where T_p is the temperature of the maximum DSC peak, ΔT is the full width at half maximum of the DTA peak.

RESULTS AND DISCUSSION

In order to determine the crystalline phase formed by thermal treatment, XRD analysis was carried on the samples. Similar XRD patterns were obtained indicating the crystallization of two major crystalline phases, wollastonite and hematite, according to the JCPDS cards (Fig. 1). While some hydroxylapatite and schorlomite were also present in sample *B*2 and *B*3, respectively.

The DSC curves of the investigated glasses at various heating rates were shown in Fig. 2. Kinetic analysis was performed by the initial temperature T_0 and the highest peak T_p of the DSC curve. The non-isothermal kinetic parameter n were shown in Table 1, which were calculated according to Eq. (13). The average values n of samples *B*1, *B*2, *B*3 were 2.21, 3.72, 3.60, respectively. The conversion degree in the range 0.1–0.7 was chosed to analyse the non-isothermal data because that the errors were relatively high at the beginning and the end of the DTA curves.

The activation energy of crystallization E and k_0 of sample *B*1 were calculated from Augis-Bennett approximation method. The curves $\ln[\beta/(T_p - T_0)]$ vs. $1/T_p$ were drawn (Fig. 3). The activation energy E was calculated from the slope while k_0 was obtained from the intercept, $E = 487.3$ kJ mol^{-1}, $k_0 = 3.294 \times 10^{22}$ min^{-1}. The value of n was optimized combined with Eq. (8), with $n = 2.0, 2.1, 2.2, 2.3, 2.4$. The results showed that $n = 2.3$ close to the actual results according to the comparison of $\alpha = \alpha(T)$ (Fig. 4). It comes out that a

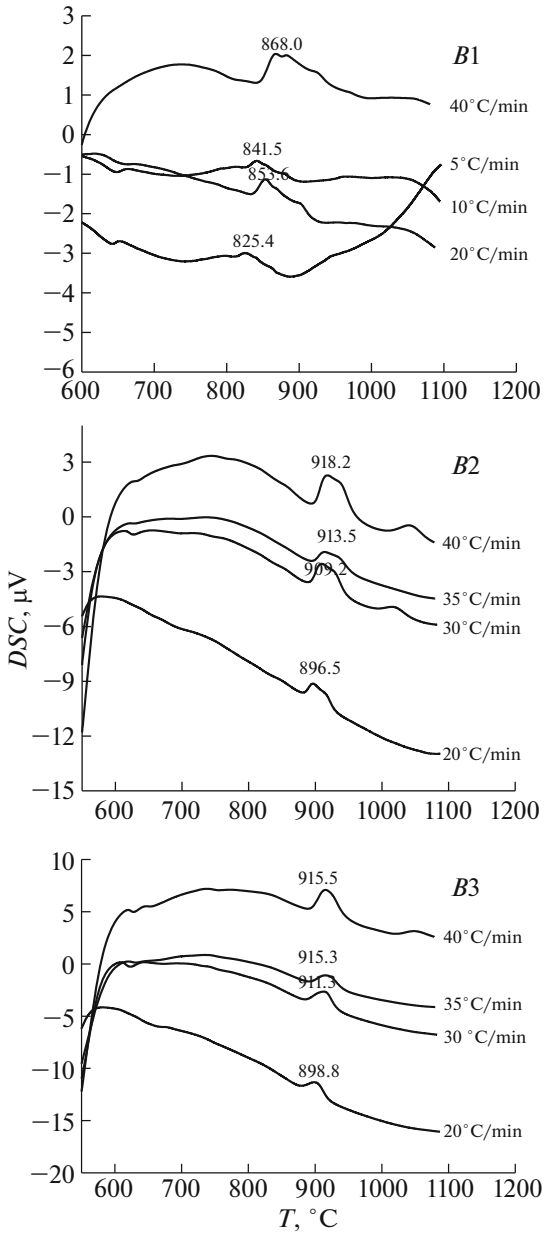

Fig. 2. DSC curves of the glass samples.

satisfactory agreement among the experimental and reconstructed $\alpha = \alpha(T)$ curves exist. However, the error of $\beta = 40$°C min^{-1} was slightly high. The reason

Table 1. The non-isothermal kinetic parameters n of the samples

*B*1		*B*2		*B*3	
β, °C min^{-1}	n	β, °C min^{-1}	n	β, °C min^{-1}	n
5	2.19	20	3.53	20	3.38
10	2.08	30	3.10	30	4.03
20	2.34	35	3.98	35	3.76
40	2.22	40	4.24	40	3.25

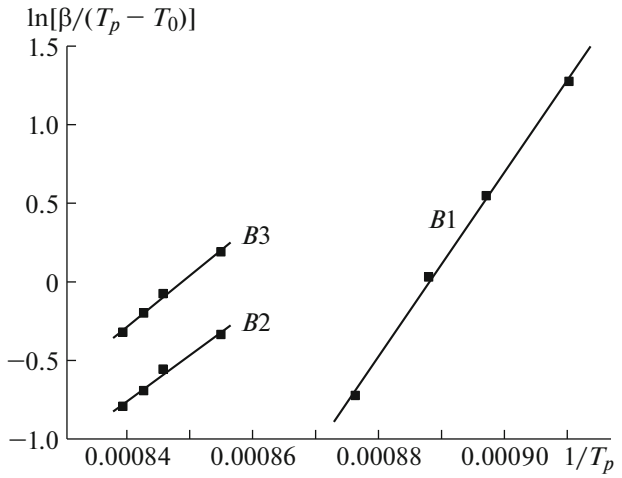

Fig. 3. The plots of $\ln[\beta/(T_p - T_0)]$ vs. $1/T_p$.

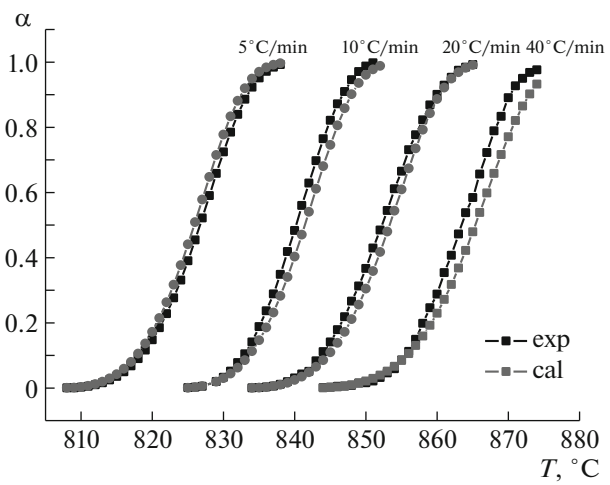

Fig. 4. The experimental and reconstructed $\alpha = \alpha(T)$ curves for kinetic model $n = 2.3$, $E = 487.3$ kJ mol^{-1}, $k_0 = 3.294 \times 10^{22}$ min^{-1}.

was that the peak was obvious with high heating rate, but the temperature with a certain lag which caused the baseline drift obviously. The kinetics model function was preliminary obtained according to Eq. (6), $f(\alpha) = 2.3(1-\alpha)[-\ln(1-\alpha)]^{0.57}$, $g(\alpha) = [-\ln(1-\alpha)]^{0.44}$.

The curves $\ln(\beta g(\alpha)/T^2)$ vs. $1/T$ was obtained corresponding to the composite integral method Eq. (10) (Fig. 5a). All points are placed around a single line for all heating rates, which indicate that the kinetics model function was suitable for Fe_2O_3–CaO–SiO_2 glass. The activation energy $E = 536.8$ kJ mol^{-1} of $B1$ was obtained from the line 5(a) ($r = 0.995$). The linear correlation coefficient r was 0.998 (Fig. 5b) while the heating rate was carried below 20°C min^{-1}, and the activation energy $E = 490.7$ kJ mol^{-1} was in good agreement with $E = 487.3$ kJ mol^{-1} obtained from Augis-Bennett approximation method.

The kinetics model function obtained from Augis-Bennett method was suitable for Fe_2O_3–CaO–SiO_2 glass according to the above results. So the activation energys and kinetic parameters of sample $B2$ and $B3$, which were listed in Table 2, were also calclated so as to investigate the effect of nucleation agent. The results showed that the glasses containing nucleation agent had lower activation energy compared to $B1$ without nucleation agent, the activation energy of glass containing nucleation agent P_2O_5 was the lowest. The Avrami exponent $n_{B1} = 2.21$ indicates one-dimensional crystallization with a constant bulk nucleation rate, while $n_{B2} = 3.72$ and $n_{B3} = 3.6$ indicates volume nucleation and three-dimensional growth mechanism [27]. A P_2O_5 and TiO_2 usually had different effect to the activation energy, TiO_2 could reduce activation energy in all the systems while P_2O_5 could reduce acti-

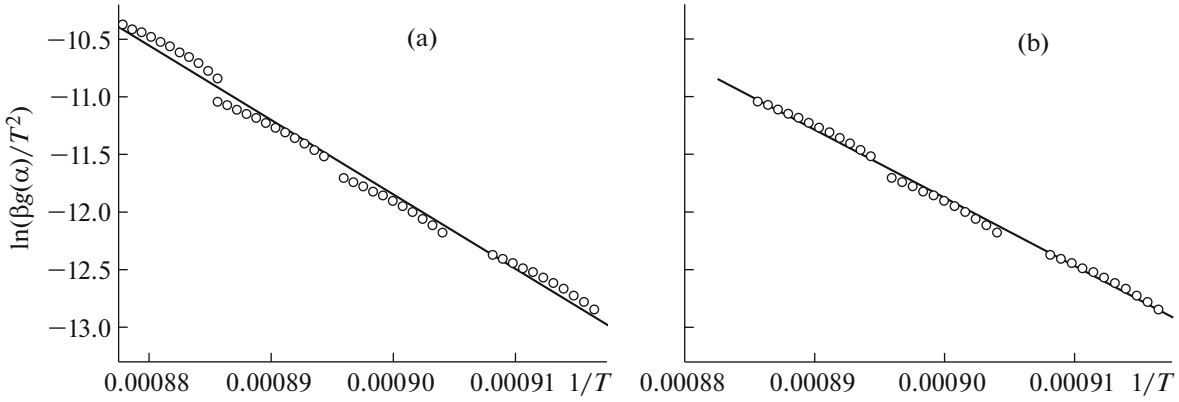

Fig. 5. The plots of $\ln(\beta g(\alpha)/T^2)$ vs. $1/T$. (a) 5°C min$^{-1} \le \beta \le$ 40°C min^{-1}; (b) 5°C min$^{-1} \le \beta \le$ 20°C min^{-1}.

Table 2. Activation energy and kinetic parameters of the samples

Sample	*B*1	*B*2	*B*3
E, kJ mol^{-1}	487.3	244.1	271.0
n	2.21	3.72	3.60

vation energy only in some systems [28]. However, both P_2O_5 and TiO_2 could reduce activation energy to similar level in Fe_2O_3–CaO–SiO_2 glass. Both of them $n \approx 4$, which indicate that they had the similar crystallization mechanism.

CONCLUSIONS

The JMA and Augis-Bennett method as well as the composite integral method were used for the analysis of the non-isothermal kinetic of Fe_2O_3–CaO–SiO_2 glass and Fe_2O_3–CaO–SiO_2 glass containing nucleation agent P_2O_5 and TiO_2. The results showed that the kinetics model of *B*1 was consistent with JMA model, whose $n = 2.3$ with one-dimensional crystallization, while the kinetics model function of Fe_2O_3–CaO–SiO_2 glass was preliminary obtained. It comes out that a satisfying agreement of these calculated curves with those experimentally obtained. The addition of nucleation agent P_2O_5 and TiO_2 could reduce the activation energy of Fe_2O_3–CaO–SiO_2 glass, which caused the crystal growth modes change from one-dimensional to three-dimensional.

This work was financially supported by the Surface Project of National Natural Science Foundation (no. 51372081), Natural Science Foundation of Zhejiang Province (LY13E020006), Medical Scientific Research Foundation of Zhejiang Province (2014PYA021) and Huzhou Science and Technology R&D Fund (2013GYB02).

REFERENCES

1. Y. K. Lee, S. B. Lee, Y. U. Kim, et al., Mater. Sci. **38**, 4221 (2003).
2. M. Miho, Lab. Invest. **23**, 176 (2004).
3. M. Akihiko and K. Katsuyuki, Clin. Exp. Metastasis **24**, 191 (2007).
4. Y. Y. Wang, B. Li, and Y. Y. Wang, Appl. Mech. Mater. **624**, 114 (2014).
5. M. Baikousi, S. Agathopoulos, and I. Panagiotopoulos, J. Sol-Gel Sci. Tech. **47**, 95 (2008).
6. M. Kamal, I. K. Battisha, and M. A. Salem, J. Sol-Gel Sci. Tech. **58**, 507 (2011).
7. A. A. S. Lopes, R. C. C. Monteiro, and R. S. Soares, J. Alloys Compd. **591**, 268 (2014).
8. M. Ghasemzadeh, A. Nemati, and A. Nozad, Ceramics-Silikaty **55**, 188 (2011).
9. E. J. C. Davim, A. M. R. Senos, and M. H. V. Fernandes. J. Therm. Anal. Calorim. **117**, 643 (2014).
10. A. Arora, E. R. Shaaban, and K. Singh, J. Non-Cryst. Solids **354**, 3944 (2008).
11. G. C. Kang. J. Mater. Sci. **36**, 1043 (2001).
12. G. O. Piloyan, I. D. Rybachikov, and O. S. Novikov, Nature **212**, 1229 (1966).
13. H. E. Kissinger, Anal. Chem. **29**, 1702 (1957).
14. J. C. Qiao and J. M. Pelletier, J. Non-Cryst. Solids **357**, 2590 (2011).
15. N. Khair and M. A. Chaudhry, J. Mater. Sci. **48**, 1368 (2013).
16. S. D. Stookey, Ind. Eng. Chem. **51**, 805 (1959).
17. A. M. Hu, K. M. Liang, G. Wang, et al., J. Therm. Anal. Calorim. **78**, 991 (2004).
18. P. E. Doherty, D. W. Lee, and R. S. Davis, Am. Ceram. Soc. **50**, 7781 (1967).
19. J. W. Cao, Y. H. Li, and K. M. Liang, Adv. Appl. Ceram. **108**, 352 (2009).
20. W. A. Johnson and R. F. Mehl, Trans. Am. Inst. Min. Metall. Pet. Eng. **135**, 416 (1939).
21. M. J. Avrami, J. Chem. Phys. **7**, 1103 (1939).
22. M. A. Gabal, Thermochim. Acta **402**, 199 (2003).
23. P. Budrugeac and E. Segal, J. Therm. Anal. Calorim. **82**, 677 (2005).
24. A. W. Coats and J. P. Redfern, Nature **201**, 68 (1964).
25. B. Jankovic and S. Mentus, Metall. Mater. Trans. A **40**, 609 (2009).
26. J. A. Augis and J. E. Bennett, J. Therm. Anal. **13**, 283 (1978).
27. K. Matusita, T. Komatsu, and R. Yokota. J. Mater. Sci. **19**, 291 (1984).
28. G. Baldi, E. Generali, C. Leonelli, T. Manfredini, G. C. Pellacani, and C. Siligardi, J. Mater. Sci. **30**, 3251 (1995).